# Enhancing Dermatological Diagnostics: An Enhanced Approach for Skin Cancer Classification Using pix2pix GAN

Adnan Afroz<sup>1</sup>, Shaheena Noor<sup>2</sup>, Shakil Ahmed Bashir<sup>3</sup>, Umair Jilani<sup>4</sup>

Dept. of Computer Engineering, Sir Syed University of Engineering and Technology, Karachi, Pakistan<sup>1</sup> Dept. of Computer Engineering, Sir Syed University of Engineering and Technology, Karachi, Pakistan<sup>2</sup> Dept. of Computer Science, FAST National University, Karachi, Pakistan<sup>3</sup>

Dept. of Telecommunication Engineering, Sir Syed University of Engineering and Technology, Karachi, Pakistan<sup>4</sup>

Abstract—Skin cancer is among the predominant forms of the disease that includes malignant squamous cell carcinoma, basal cell carcinoma, and melanoma that is characterized by aberrant melanocyte cell development. Frequent screenings and examinations enhance the prognosis for people with skin cancer. Sadly, a lot of patients with skin cancer are not diagnosed until the condition has progressed past the point at which treatment is effective. Deep learning techniques in computer vision have made impressive strides, but issues like class imbalance and a lack of data still hinder the autonomous identification of skin conditions. A solution to address these problems is the implementation of GAN, which is capable of synthesizing realistic data. In this paper, a deep learning GAN model for image synthesis utilizing the pix2pixHD integrated with Convolutional Neural Network (CNN) classifier approach is used to perform skin cancer classification. To categorize three forms of skin cancer benign or malignant. The proposed pix2pixHD GAN is a novel method for utilizing pertinent skin lesion information for generation of high-quality synthesized dermoscopic image and conduct skin lesion classification performance with improved accuracy. Realistic images were created using a U-Net-based generator and PatchGAN discriminator with custom CNN architecture to classify three forms of cancer. With remarkable accuracy of 87.65% (MEL), 91% (BCC), and 89.85% (SCC) and other performance parameters indicate that GAN pix2pixHD Classifier model has promising results in classification. These findings demonstrate the Classifier's ability to produce and correctly identify high-quality skin lesion images, indicating its potential as a deep learning-based medical image analysis tool.

Keywords—Deep learning; skin cancer; generative adversarial network; pix2pixHD; classification

# I. Introduction

The human body's most important and sensitive organ, the skin, acts as the body's main defense against the environment and is essential for shielding the body from dangerous UV rays and illnesses. But because it is the outermost layer, it can get a variety of ailments, including skin cancer, which is one of the most prevalent cancers in the world [1] Many people are suffering from different types of skin cancer. In the year 2021 there were approximately 6.64 million new cases of skin cancers worldwide, encompassing both melanoma and non-melanoma types [2]. The stats provided that in year 2022, an estimated

330,000 new cases of melanoma were diagnosed globally, with nearly 60,000 deaths attributed to the disease [3].

As per study, in the US in 2019, about 100,000 new cases was found and 7,000 people will die. Lucky for us, melanoma treatment works much better when it was found early; it has a 92% 5-year survival rate, but only 26% when it was found later. So, finding and diagnosing melanoma as soon as possible is very important [4].

Current improvements in computer vision using Artificial Intelligence (AI) have improved diagnosis and detection approaches for fatal malignant skin conditions. Skin cancer diagnosis has always relied on manual screening and physical inspection. Dermatologists' procedures for visual inspection and evaluating of disease images are challenging, unreliable, and mistake prone[4]. The cancerous pixels must be recognized correctly to do investigation, interpretation, and comprehension of skin lesion images. This is challenging for the reasons stated below.

- Hair, veins, lubricants, bubbles, and various other clutter may be present in lesions on the skin images, interfering with the segmentation process.
- A lack of contrast between the adjacent skin and the lesion area also makes precise segmentation of the lesion difficult.
- Skin lesions typically vary in size, form, and color, limiting the efficiency of procedures in obtaining a greater accuracy degree level.

Skin lesions typically vary in size, form, and color, limiting the efficiency of procedures in obtaining a greater accuracy degree level. Due to this, demonologist find manual diagnosis challenging and necessitates the implementation of computerized diagnostic for analysis of skin lesion in making fast decisions. It has helped specialists make more precise and rapid recommendations concerning but its most threaten type Melanoma, have a very high death rate, but they are easy to treat if they are found early [4].

Over the years, different automated methods have been used to find and diagnose skin cancer. This is how medical imaging analysis is generally done: by using various dermoscopic image processing techniques. In general, the complete procedure of finding melanoma cancer can be broken down into four essential steps:

- Preliminary image processing.
- Segmentation of images.
- Extraction of features.
- Classification of cancerous tumors.

Some of the other techniques used in preliminary processing include adjusting contrast and sharpness, morphological operations, binarization, data augmentation and colour greyscaling. Noise and other irregularities are taken out of images at this stage. Resizing images makes sure that they are all the same size, which also makes computations easier. Segmentation of skin images run right after pre-processing, of images, separates the diseased area from the healthy meat to get the region of interest

It divides healthy tissue prior to collecting lesions' features for suitable diagnosis. Skin lesion analysis for the identification of melanomauses thresholds, clustering, edge and region-based, and ABCDE segmentation Algorithm. Such methods struggle to successfully partition the Melanoma region because of the complicated visual appearance of the skin lesions [5].

The majority of current research on skin cancer classification uses either traditional CNN architectures or GAN-based data augmentation for binary classification, often with poor image quality and insufficient management of data imbalance. This research fills this gap by combining a CNN classifier with pix2pix GAN to improve lesion representation and diagnostic performance for BCC, SCC, and melanoma.

### II. METHODS

## A. Skin Cancer Diagnosis Through Deep Learning

The fine-grained variety of skin lesion appearances makes the task of classifying skin lesions difficult. As highperformance computing has advanced and massive datasets have emerged, deep learning techniques have demonstrated significant promise in a variety of image processing applications. Additionally, the most deployed deep learning convolutional neural network (CNN) performs end-to-end training using labels and image pixel input. CNN is better than the hand-crafted method in automatically extracting salient characteristics from the input data. CNN used for the first time in 1995 and utilized for analysis of medical imaging [6]. To train a deep CNN model with strong generalization capabilities, sufficient labelled data is needed. However, there aren't many publicly accessible data points for classifying skin lesions. The model transfer technique through transfer education are the main categories of classification [7].

The 129,450 clinical images were used to fine-tune the GoogleNet Inception v3 CNN architecture, which had been pretrained on the ImageNet dataset. With 2,032 disease types serving as its leaf nodes, and tree-structured taxonomy-based dataset is arranged. A partitioning algorithm is used to define the training classes based on these leaf nodes. Two binary classification challenges were used to evaluate the CNN model's performance with that of 21 dermatologists. The findings

demonstrate that in certain skin cancer classification tasks, artificial intelligence has surpassed human experts. Numerous follow-up researchers have been drawn to this seminal work [8].

Researcher looked into using artificial intelligence and dermatologists to classify skin lesions [9]. The authors generated two sets of classification results using a ResNet50 model [10]. The XGBoost method was then used to merge the findings. Artificial intelligence and human decision-making together demonstrated superiority over separate systems [11].

Research has been conducted and demonstrated that augmented data is beneficial for accuracy by accurate classification and preventing overfitting by training a 4-layered CNN model with to distinguish benign skin lesions from melanoma using both normal and supplemented datasets [12].

By training two dual deep CNNs and allowing them to support one another, a unique skin lesion categorization model was created [12]. The ISIC 2016 Challenge dataset yielded state-of-the-art results for the suggested model [13].

Data synthesis, a more advanced technique for data augmentation, is intriguing and well-liked. Variational autoencoders (VAEs) [14] and generative adversarial networks (GANs) are the two most used methods for data synthesis [15]. In addition to classifying the input data into distinct classes, the WGAN can produce 64 x 64 images. The suggested approach used just 140 labelled images from the ISIC 2016 Challenge dataset, yielding an average precision score of 0.424 [16].

Research was conducted and presented a deeply differentiated GAN (DDGAN) with the goal of improving the resolution of produced image [17]. In order to demonstrate that DDGAN [18] and LAPGAN [19] that both can learn the distributed datasets and synthesize samples that looks like realistic, the authors created realistic-looking 256 x 256 skin lesion image and compared them.

GAN for image synthesis using pix2pixHD. They synthesize maps and semantic maps rather than creating images from random noise. The suggested pix2pixHD GAN is a unique approach to using the relevant skin lesion information for synthesizing high-quality image, and it is somewhat conducive to skin lesion classification performance, even if it needs annotated data to produce images, but this approach only characterized two types of skin cancer benign or melanoma [20].

#### B. Dataset

We require certain masks that demonstrate the presence or absence of clinically significant skin lesion patterns to train and evaluate pix2pix.

These masks may be found among the 2,601 images from the 2018 ISIC training dataset[21]. The segmentation masks for the same lesions, which are utilized to create instance and semantic maps, were acquired via the 2018 ISIC Challenge[21]. To train 2,056 images and test 545 images, we divided the data for three different classes. The details of divided data available in Table I.

A resilient adversarial learning objective function, a patch GAN discriminator architecture, and a generator with U-net are used in the pix2pix network that is a conditional image-to-image

translation GAN. The network was able to operate with high-resolution samples as shown in Fig. 1.

Differentiating between Basal Cell Carcinoma, Melanoma and Squamous Cell Carcinoma is in skin categorization process. Conventional CNN-based classifiers use used that classify in between three dermoscopic images to directly learn features.

Pix2pix model is used to generate synthetic images and trained to improve dermoscopic images as shown in Fig. 2(a) and 2(b). The CNN classifier learn features from these generated images and classify the three skin cancer types. CNN classifier

has total to 115,232 trainable parameters, max pool and fully connected layer at output.

TABLE I. DATA FOR TRAINING AND TESTING

Image Class	Training	Testing	Total
Basal Cell Carcinoma(BCC)	679	188	867
Melanoma(MEL)	700	167	867
Squamous Cell Carcinoma(SCC)	677	190	867
Total	2056	545	2601

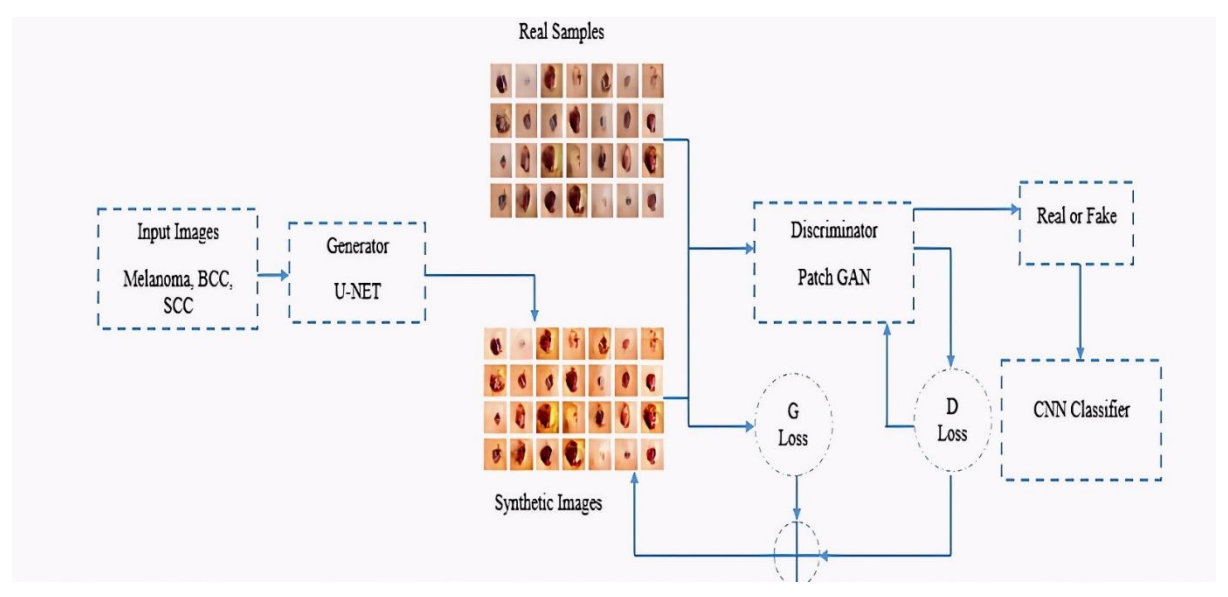


Fig. 1. Pix2pix GAN: Image generation and classification.

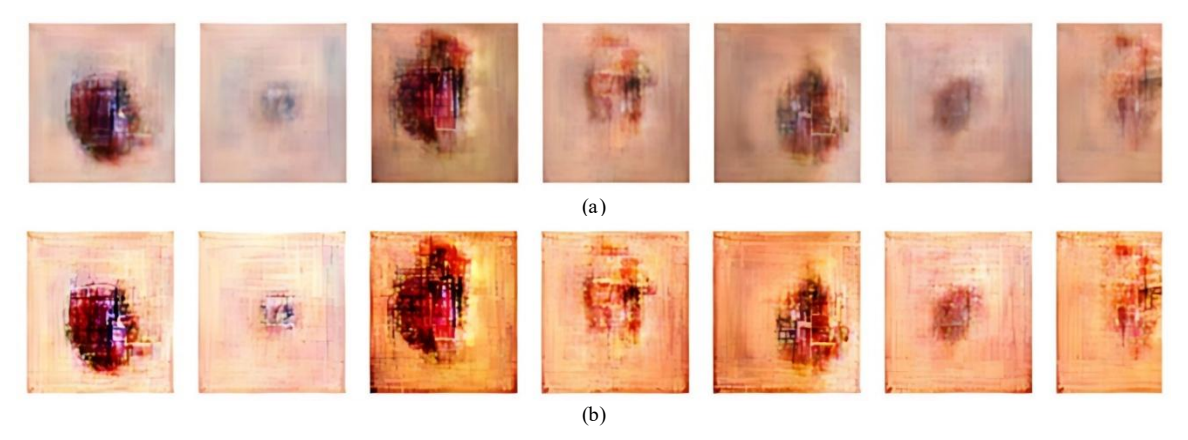


Fig. 2. (a) Original image input from ISIC 2018 dataset, (b) High resolution synthetic images generated from pix2pix GAN.

A U-Net design, which is useful for maintaining spatial information essential for medical image, is commonly used by the pix2pix generator. The discriminator is a PatchGAN, which helps the model concentrate on texture and fine features by classifying tiny patches of the Image instead of the entire image. Adversarial loss and L1 loss the pixel-by-pixel difference between the produced Image and the ground truth are used in tandem to train the pix2pix model. Segmentation masks or diagnostic labels can be used to direct the learning process for melanoma tasks. After training, the pix2pix output is utilized as a preprocessing step for an independent classification network

or directly for diagnosis. In certain instances, the produced image alone can be sufficiently interpreted to help doctors make diagnoses.

The generator is encouraged to provide outputs that are identical to actual images by the adversarial loss as shown in Eq. (1):

$$LcGAN(G,D) = Ex, y[logD(x,y)] + Ex, z[log(1 - D(x,G(x,z)))]$$
(1)

An L1 loss as shown in Eq. (2) is used to guarantee that the produced images near the ground truth that improve pixel level accuracy and decrease blurriness.

$$\lambda \mathcal{L}_{l,1}(G) = \operatorname{E} x, y[\parallel y - G(x) \parallel 1] \tag{2}$$

Realism is guaranteed by the GAN loss. The input's fidelity is guaranteed by the L1 loss. When combined, they yield results that are correct semantically and believable visually as shown in Eq. (3):

$$G^* = \arg\min_{G} \max_{D} L_{C} GAN(G, D) + \lambda \mathcal{L}_{L1}(G)$$
 (3)

The model architecture consists of generator with U-Net attention, input of RGB image of 256 x 256, activation function

of ReLU in encoder, LeakyReLU in decoder, and Tanh at final output as illustrated in Fig. 3.

The U-Net architectural design is for the purpose of medical image segmentation. It has a symmetric structure that constitutes an encoder and decoder: the encoder will collect contextual information through down-sampling, while the decoder restores fine-grained details by up-sampling. A distinguishing feature that gives U-Net its advantage is the presence of skip connections between symmetric layers of the encoder to the decoder. These connections help in retaining some spatial information that could be lost during down-sampling and make U-Net particularly good at tasks that need high localization accuracy, such as boundary delineation in medical images [22].

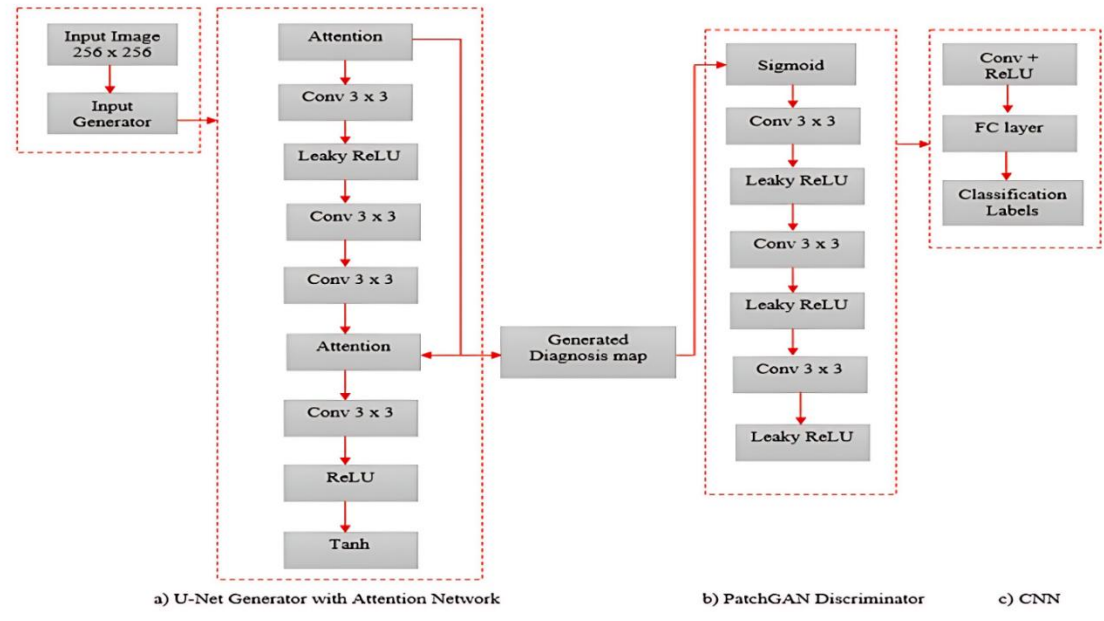


Fig. 3. Pix2pix GAN architecture with U-Net generator and CNN as classifier.

The U-Net architecture acts as a generator in a pix2pix GAN setup developed for medical-image-segmentation tasks. First, dermoscopic images (256×256 pixels) are fed into the encoderdecoder structure. The encoder successively down-samples the image, using convolutional layers with ReLU activation and batch normalization (except for the last layer), extracting deeper features while reducing spatial resolution. With each downsampling step, the number of feature channels is increased so that the model can learn complex patterns. The decoder upsamples these features to reconstruct the image at the original resolution using transposed convolutions and LeakyReLU activations. A vital design consideration is the use of skip connections between corresponding encoder and decoder layers so that fine-grained features from the earlier layers can directly influence the output. Such preservation of spatial details minimizes information loss in the down-sampling process. Finally, the single-channel output  $(256 \times 256 \times 1)$  representing the diagnosis or segmentation map is activated using the Tanh function, constraining pixel values to the range of [-1,1]. This U-Net generator is pivotal to attaining realistic and spatially accurate outputs in the pix2pix GAN pipeline [22]. The inclusion of attention in this way improves both interpretability of the model and its segmentation accuracy, especially in applications dealing with skin cancer imaging. The model is therefore facilitated in providing more accurate and realistic segmentations of lesions in aiding clinicians in suspicious area identification. Visualizing these attention maps presents additional insight into what the model considers most relevant for diagnostic purposes.

Linear transformation performed in Attention network achieved through encoder feature map in Eq. (4):

$$x \in R^{\wedge}(Fx \times H \times W)$$
 (4)

The decoder feature map is achieved through gating signal along with skip connections to produce feature map in Eq. (5).

$$g \in R^{\wedge}(Fg \times H' \times W') \tag{5}$$

Applying the linear projections on both equations through convolution shown in Eq. (6) and (7).

$$\theta x = W(x) x \tag{6}$$

$$\phi g = W (g) g \tag{7}$$

Two inputs are projected, added and passed through activation function ReLU that helps in learning the non-linear projections between encoder and decoder as shown in Eq. (8).

$$\psi = \text{ReLU} (\theta \ x + \phi \ g)$$
 (8)

Scalar map is needed to produce attention network for knowing the important spatial regions by using sigmoid as activation function and convolution network as shown in Eq. (9).

$$\alpha = \sigma(W \psi \psi + b \psi)$$
 (9)

The discriminator usually uses a PatchGAN architecture, The discriminator usually uses a PatchGAN architecture, which works as a Markovian discriminator by assessing the realism of tiny, overlapping patches 70×70 rather than the full image for balanced realism & accuracy. Because it enforces for high accuracy, this localized technique is especially well-suited for medical imaging jobs where fine-grained characteristics like lesion boundaries, pigmentation, and texture changes are crucial for diagnosis. In order to encourage the generator to generate anatomically correct and spatially coherent outputs, PatchGAN slides a neural classifier over the Image and classifies each patch as real or false. This results in more realistic lesion shapes and clearer borders, both of which are necessary for accurate skin cancer segmentation and detection. The Adam Optimizer is used with tuned parameters. We tried different sets of values for different parameters but there is problem of fast convergence. The values of  $\beta 1$  and  $\beta 2$  are set to stabilize the training process as available in Table II:

TABLE II. TUNED PARAMETER FOR PIX2PIX GAN

Parameter	Value	
Input Image Size	256x256	
Batch Size	16	
Learning Rate (Generator)	0.0002	
Learning Rate (Discriminator)	0.0001	
Optimizer	Adam	
β1	0.5	
Epochs	200	

# III. PERFORMANCE EVALUATION

Classification purposes in the health domain wants great sensitivity as it signifies the measure of the system's value. Sensitivity is stated as Eq. (10):

$$Sensitivity/Recall = \frac{(TP)}{(TP+FN)}$$
 (10)

Precision represents the ratio of accurately labels that are classified truly positive, which is stated as Eq. (11):

$$Precision = \frac{(TN)}{(FP + TN)} \tag{11}$$

Accuracy calculates the sum of appropriately classified skin lesions divided by the total number of skin lesions, which is stated as Equation 12 and F1-score in Eq. (13):

$$Accuracy = \frac{(TP+TN)}{(TP+FN)+(FP+TN)}$$
 (12)

$$F1 Score = \frac{(2*TP)}{(2*TP+FN+FP)}$$
 (13)

#### IV. RESULTS AND DISCUSSION

We train a skin classification network with both synthetic and actual training sets to assess the entire set of synthetic images. Then, we compare the area images. For this comparison, we employ three distinct synthetic images created with our version of pix2pix that use both instance and semantic maps are called instances.

Only semantic label maps are used to produce semantic samples, whereas our conditional PGAN is used to generate PGAN samples. The best synthetic samples are those that are produced using instance maps. The findings for synthetic images confirm that they include characteristics that indicate whether a lesion is MEL, BCC and SCC. Furthermore, the findings imply that the created images have characteristics that go beyond what is found in the actual images. The predicted output is shown Fig. 4 that has three classified outputs.

The performance evaluation for our implemented CNN classifier is available in Table III. These values confirm that the model maintains strong precision-recall performance, especially for BCC, with slightly more variability in MEL and SCC. The implemented model reveals that the performance evaluators are nearly equal to accuracy for predicted classes.

TABLE III. PERFORMANCE EVALUATORS FOR PIX2PIX GAN AND CNN AS

Class	Accuracy	Precision	Recall	F1-Score
BCC	91%	93%	91%	92%
MEL	87.65%	89.18%	88.06%	88.1%
SCC	89.85%	87.23%	90%	88%

In order to validate the result, we have implemented the dataset on different deep learning models and the results are available in Table IV. For different models the recall, F1 and precision values are close to accuracy for VGG-16 MobileNet-V2 and InceptionV3 model that depicts the accuracy of generated synthetic images.

TABLE IV. PERFORMANCE EVALUATORS FOR DIFFERENT DEEP LEARNING MODELS

	VGG-16[23]			
Class	Accuracy	Recall	F1-Score	Precision
BCC	84.83%	83.27%	83.42%	83.62%
MEL	82.18%	79.83%	78.30%	80.63%
SCC	83.78%	81.00%	79.00%	80.31%
		Mobile	Net-V2[24]	
BCC	79.58%	79.30%	78.20%	80.97%
MEL	84.63%	82.02%	77.23%	82.89%
SCC	82.58%	80.28%	80.00%	81.00%
		Incepti	onV3[25]	
BCC	82.13%	80.45%	82.64%	80.27%
MEL	83.02%	81.75%	82.33%	82.42%
SCC	85.89%	85.00%	83.97%	83.14%

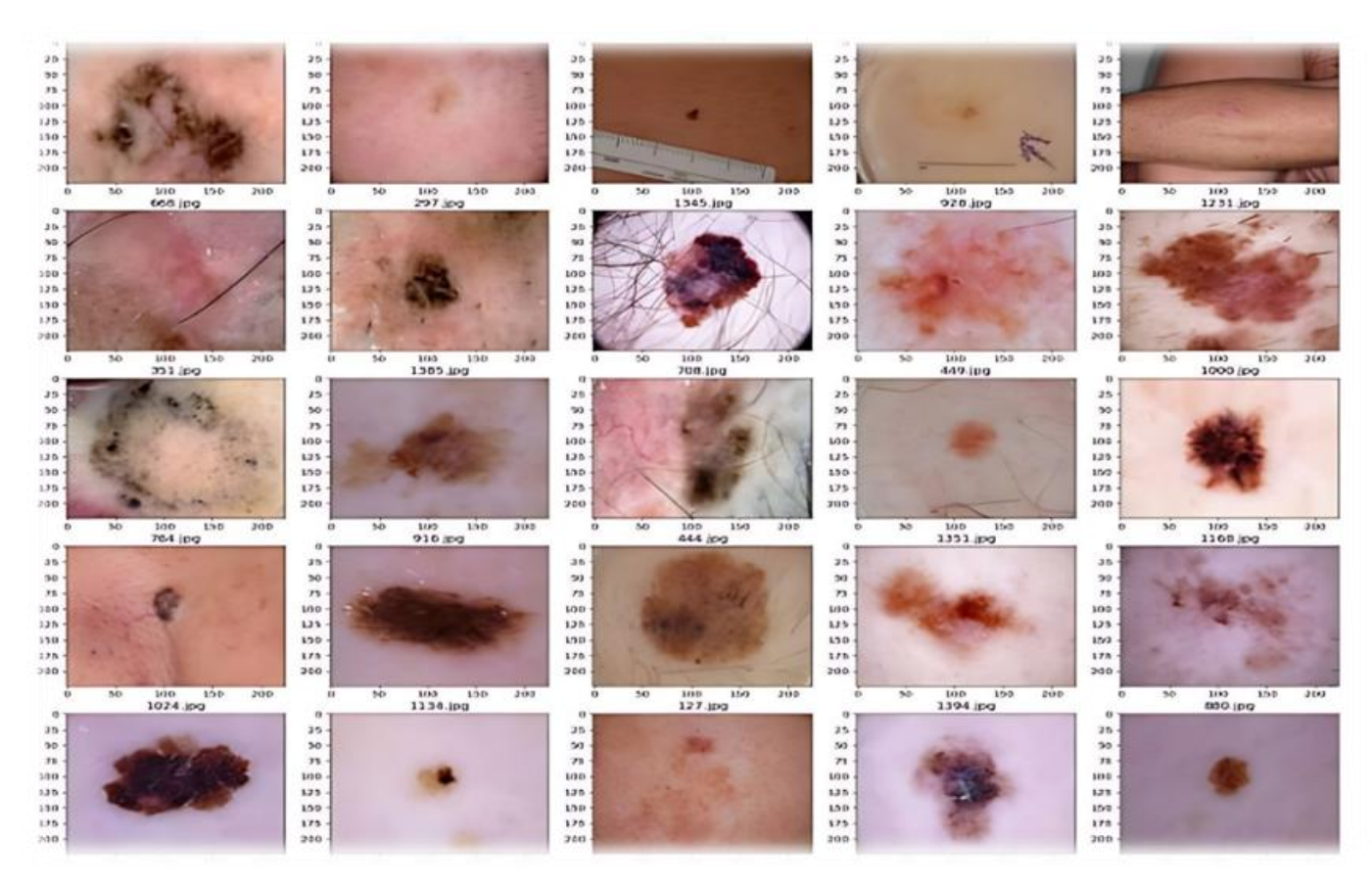


Fig. 4. Three classified outputs after CNN classification.

The model was trained on CPU 7th Generation core i-7 Intel processor, with 16 gigabytes (GB) of NVDIA GeForce GTX 1080 with 8 GB of RAM make up the system's Graphical Processing Unit (GPU). The confusion matrix for our implemented CNN classifier for three types of skin cancer for classification is shown in Fig. 5.

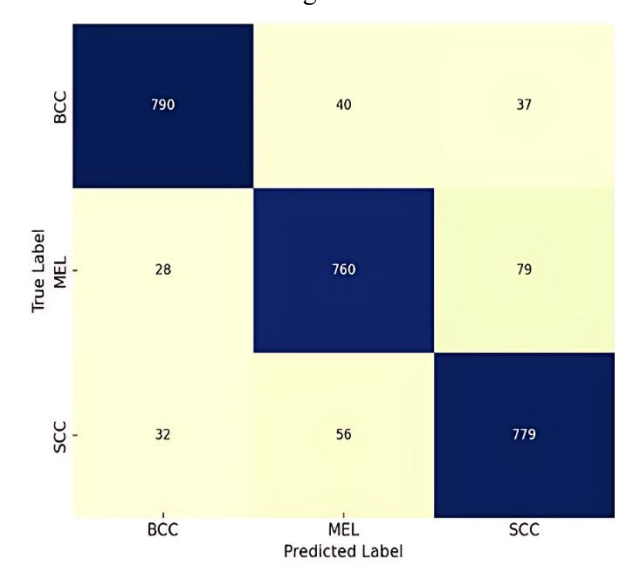


Fig. 5. Confusion matrix for classification of MEL, BCC and SCC through CNN classifier.

In order to validate the result, we have implemented the dataset on different deep learning models and the results are available in Table IV. ROC and Precision-Recall curves for MEL, BCC and SCC are shown in Fig. 6(a) and Fig. 6(b). For different models the recall, F1 and precision values are close to accuracy for VGG-16, MobileNet-V2 and InceptionV3 model that depicts the accuracy of generated synthetic images.

Results clearly shows that our proposed hybrid method, implementing pix2pix GANs with CNNs, predicts 91% accuracy on BCC, 87.65% on MEL and 89.85% on SCC using the ISIC-2018 dataset compared with typical CNN models like VGG-16, MobileNet-V2, and InceptionV3 by roughly 5 to 10% with reduced computational power and enhanced multi-class skin lesion classification. Table V also displays the comparison-based classification performance accuracy results of other authors' related work.

TABLE V. CLASSIFICATION PERFORMANCE ACCURACY FOR EXISTING RESEARCH

Author	Model	Classes	Accuracy
[8]	Inception v3 CNN	2	85%
[9]	Hybrid	2	88%
[12]	Synergic CNN	2	82-85%
[17]	MelanoGANs	2	<85
[20]	pix2pix GAN	2	85

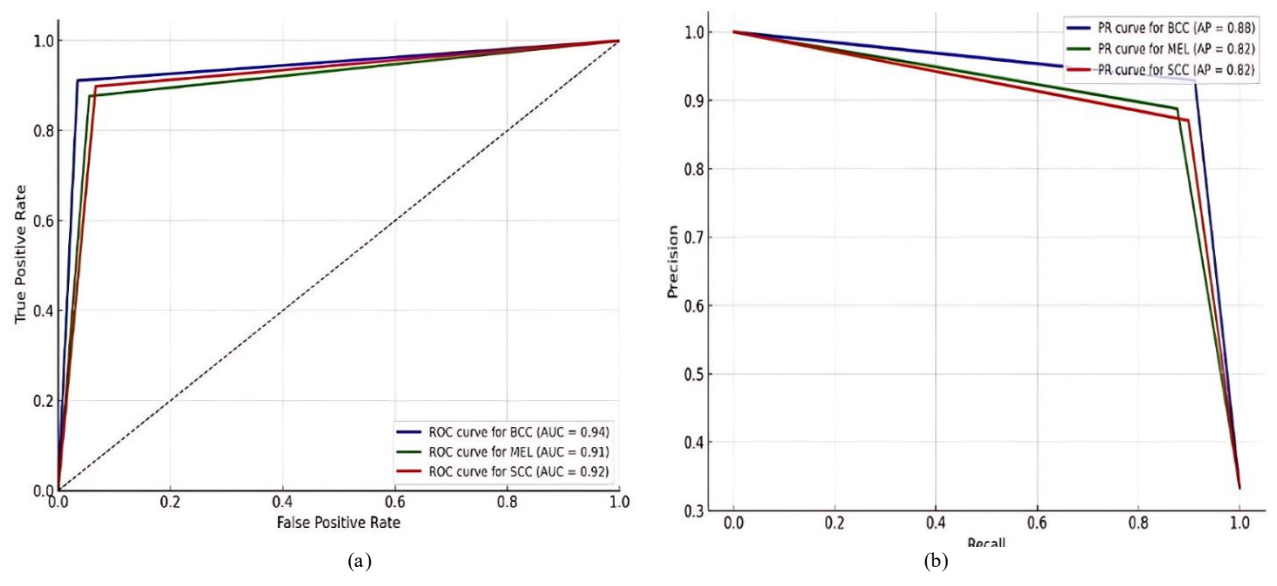


Fig. 6. (a) ROC curves for MEL, BCC and SCC, (b) Precision-recall curves for MEL, BCC and SCC.

## V. CONCLUSION

Medical imaging is rapidly being driven by hybrid deep learning frameworks that combine generative and discriminative models. This research work used a pix2pix GAN with a U-Net generator and PatchGAN discriminator, together with a customized CNN classifier, to improve the classification of melanoma (MEL), basal cell carcinoma (BCC), and squamous cell carcinoma (SCC). The model efficiently controlled data imbalance and variability by synthesizing high-resolution dermoscopic images, reaching classification accuracies of 91% (BCC), 87.65% (MEL), and 89.85% (SCC), outperforming other models such as VGG-16, MobileNet-V2, and InceptionV3. These findings highlight the potential for GANaugmented classification to increase diagnostic performance and robustness. A strong transition toward clinically deployable, high-precision diagnostic systems in dermatology is shown by this, which is consistent with current research trends that emphasize data augmentation and multimodal learning.

# VI. CONFLICT OF INTEREST

The authors declare that there is no conflict of interest regarding the publication of the paper.

#### REFERENCES

- L. Wei, Zhang, Y., & Liu, J, "Enhanced skin cancer diagnosis using optimized CNN architecture," BMC Medical Imaging, vol. 24, no. 1, pp. 15-25, 2024.
- [2] Z. Y. Zhou L, Han L, Xie Y, Wan M. Global, "Regional, and national trends in the burden of melanoma and non-melanoma skin cancer: insights from the global burden of disease study 1990-2021," Sci. Rep vol. 15, no. 1, 2025, doi: doi: 10.1038/s41598-025-90485-3.
- [3] I. A. f. R. o. Cancer. "IARC marks Global Non-Melanoma Skin Cancer Awareness Day." https://www.iarc.who.int/cancer-type/skin-cancer (accessed.
- [4] R. Gupta, & Sharma, "Skin cancer detection and classification using neural networks: A systematic review," Journal of Engineering and Computer Innovations, vol. 5, no. 2, pp. 45-60, 2024.
- [5] S. S. G. Pellacani, "Comparison between morphological parameters in pigmented skin lesion images acquired by means of epiluminescence surface microscopy and polarized-light videomicroscopy," Clin. Dermatol, vol. 20, no. 3, pp. 222–227, 2002.

- [6] H. P. H Kittler, K Wolff, M Binder, "Diagnostic accuracy of dermoscopy," The Lancet Oncology, vol. 3, no. 3, pp. 159-165, 2022, doi: https://doi.org/10.1016/S1470-2045(02)00679-4.
- [7] S. Y. Pan, "Q.: A survey on transfer learning," IEEE Transactions on Knowledge and Data Engineering, vol. 22, no. 10, pp. 1345-1359, 2010.
- [8] A. Esteva, Kuprel, B., Novoa, "Dermatologist-level classification of skin cancer with deep neural networks," Nature vol. 542, pp. 115–118 2017.
- [9] J. S. U. Achim Hekler, Alexander H. Enk, Axel Hauschild, Michael Weichenthal, R.C. Maron, "Superior skin cancer classification by the combination of human and artificial intelligence," European Journal of Cancer, vol. 120, pp. 141-121, 2019, doi: https://doi.org/10.1016/j.ejca.2019.07.019.
- [10] K. He, X. Zhang, S. Ren, and J. Sun, "Deep residual learning for image recognition," in Proceedings of the IEEE conference on computer vision and pattern recognition, 2016, pp. 770-778.
- [11] C. G. T.Chen, "XGBoost: a scalable tree boosting system," arXiv:1603.02754, 2016.
- [12] J. Zhang, Y. Xie, Q. Wu, and Y. Xia, "Skin lesion classification in dermoscopy images using synergic deep learning," in Medical Image Computing and Computer Assisted Intervention—MICCAI 2018: 21st International Conference, Granada, Spain, September 16-20, 2018, Proceedings, Part II 11, 2018: Springer, pp. 12-20.
- [13] N. C. F. C. D. Gutman, E. Celebi, B. Helba, M. Marchetti, N. Mishra, A. Halpern, "Skin lesion analysis toward melanoma detection: a challenge at the international symposium on biomedical imaging (ISBI) " arXiv:1605.01397, 2016.
- [14] D. P. Kingma and M. Welling, "Auto-encoding variational bayes," ed: Banff, Canada, 2013.
- [15] I. J. Goodfellow et al., "Generative adversarial nets," Advances in neural information processing systems, vol. 27, 2014.
- [16] J. T. Springenberg, "Unsupervised and semi-supervised learning with categorical generative adversarial networks," arXiv:1511.06390, 2015.
- [17] S. A. C.Baur, N.Navab, "MelanoGANs: high resolution skin lesion synthesis with GANs,," arXiv:1804.04338, 2018.
- [18] L. M. A. Radford, S. Chintala, "Unsupervised representation learning with deep convolutional generative adversarial networks," arXiv:1511.06434, 2015.
- [19] E. L. Denton, S. Chintala, and R. Fergus, "Deep generative image models using a @ laplacian pyramid of adversarial networks," Advances in neural information processing systems, vol. 28, 2015.
- [20] F. P. A.Bissoto, E.Valle, S.Avila, "Skin Lesion Synthesis with Generative Adversarial Networks," arXiv:1902.03253, 2019.

- [21] A. K. (Owner). Skin Cancer ISIC. [Online]. Available: https://www.kaggle.com/datasets/nodoubttome/skin-cancer9-classesisic
- [22] F. P. Alceu Bissoto, Eduardo Valle, Sandra Avila, "Skin Lesion Synthesis with Generative Adversarial Networks," arXiv:1902.03253, 2019, doi: https://doi.org/10.48550/arXiv.1902.03253.
- [23] K. Djaroudib, P. Lorenz, R. Belkacem Bouzida, and H. Merzougui, "Skin Cancer Diagnosis Using VGG16 and Transfer Learning: Analyzing the Effects of Data Quality over Quantity on Model Efficiency," Applied Sciences, vol. 14, no. 17, p. 7447, 2024. [Online]. Available: https://www.mdpi.com/2076-3417/14/17/7447.
- [24] H. Cheng, J. Lian, and W. Jiao, "Enhanced MobileNet for skin cancer image classification with fused spatial channel attention mechanism," Scientific Reports, vol. 14, no. 1, p. 28850, 2024/11/21 2024, doi: 10.1038/s41598-024-80087-w.
- [25] K. S. K. B. Swathi, S. S. Chakravarthi, G. Ruthvik, J. Avanija and C. C. M. Reddy, "Skin Cancer Detection using VGG16, InceptionV3 and ResUNet," presented at the 4th International Conference on Electronics and Sustainable Communication Systems (ICESC), 2023.